Laser-wavelength dependence of the picosecond ultrasonic response of a NiFe/NiO/Si structure

C. A. C. Bosco, A. Azevedo, and L. H. Acioli
Departamento de Física—Universidade Federal de Pernambuco, 50670-901 Recife, Pernambuco, Brasil
(Received 20 December 2001; revised manuscript received 16 April 2002; published 23 September 2002)

Ultrafast optical excitation and detection of acoustic phonons has been used to analyze ultrathin films composed of NiFe/NiO/Si which are important for applications in magnetic storage and processing. Results are presented on the wavelength dependence of the ultrasonic response of the thin NiO film and bulk Si. Significant changes are observed between detection using the fundamental and the second harmonic of the femtosecond laser as the probe beam. Beatings between low order longitudinal phonons in the NiO layer are observed and measurements of its refractive index and absorption coefficients are performed.

DOI: 10.1103/PhysRevB.66.125406 PACS number(s): 78.47.+p, 81.70.Cv, 78.20.−e

I. INTRODUCTION

Ultrafast optical techniques have long been demonstrated to be a very powerful technique to excite and probe short pulses of sound waves in the hundreds of GHz domain in many different kinds of samples.[1–5] As these pulses are of very small spatial extent they have proven useful for determining the thickness of ultrathin samples. More recently it was shown to be possible to experimentally study the dispersion relations of longitudinal phonons in periodic structures,[6–8] deviations from a linear dispersion relation in bulk samples,[9] and the generation of acoustic solitonic pulses.[10]

The primary step of an ultrafast optical excitation of longitudinal acoustic waves involves the absorption of a pump pulse, usually through intraband or interband electronic transitions in a metal where light has a small penetration depth. The pump pulse creates a nonuniform spatial distribution of hot electrons determined by the absorption coefficient of the sample. As has been well established by transient pump-probe spectroscopy,[11–14] within a few picoseconds the excess energy of the electron system is transferred to the lattice via electron-phonon coupling, at the same time that diffusion processes take place.[15] The result is that strong temperature gradients are established, originating strain waves that propagate into the sample, producing changes in the real and imaginary parts of the dielectric constant to which the probe pulse is sensitive. The signal is detected as a change in the reflectivity of the sample and, as shown recently, it may depend strongly on the probe's wavelength.[16] Another parameter that plays an important role is the penetration depth of the probe pulse. In experiments with transparent materials it has been demonstrated that a thin metallic film may be used as a transducer, in order to launch the strain wave into an underlying sample of interest.[15] The oscillations detected in the transparent medium depend primarily on the speed of sound v_s, and the refractive index at the probe's wavelength, $n(\lambda_{probe})$.

If strain waves are excited in thin film structures with different acoustic impedances, secondary strain waves are created and reflected back and forth between these interfaces. Interesting effects such as phonon confinement may be observed if the film thickness is small compared to the wavelength of the excited phonons.[17] More importantly for the regime we study here, the thickness of a layer determines the spacing between the acoustic modes it supports.

Ultrafast reflectivity measurements in NiO and Si within a structered thin film sample of NiFe/NiO/Silicon substrate are reported. The structures we study are important for applications in magnetism,[18] and NiO thin films are also of importance for gas sensing applications.[19–21] The samples for which the measurements were performed are schematically shown in Fig. 1, where a thin NiO layer is sandwiched between a NiFe film and bulk Si. The NiFe plays the role of a transducer, where the pump pulse is absorbed. Although the NiO layer is not transparent, it is sufficiently thin to be important to consider its mode structure, and the observation of beatings between a small number of neighboring acoustic modes in the NiO layer is reported. These modes are selected by a thickness dependent filtering function, and we present results of calculations that support our interpretation of the data. We argue that in our experimental situation this is inherent to the detection process and has little influence of the shape of the strain pulse. The measurements involve either a single- or dual-wavelength time-resolved pump-probe technique, with a femtosecond Ti:sapphire laser as the source. As previously reported by other authors,[16] we have also observed wavelength dependent piezo-optic coupling of NiO when the probe pulse photon energy is doubled. For smaller variations of the probe's photon energy we have determined the dependence of the central frequency of the observed oscillations with wavelength, obtaining the dispersion of the refractive index of the NiO films.

II. ACOUSTIC PULSE EXCITATION AND DETECTION

To compute the reflectivity changes of the sample shown in Fig. 1, we recall that the NiFe works as a transducer that launches a strain pulse into the next layer. Its thickness is typically 10 nm, and at a pump wavelength of approximately 800 nm, for which the experiments described here were performed, the penetration depth in this layer is of the same order. A fraction of the incident pump pulse is therefore transmitted into the next layers. As will be seen later from our experimental results, despite this possibility of leakage of the pump pulse, the strain pulse $\eta(z,t)$ is indeed launched by the NiFe transducer into the NiO film. The total transient reflectivity variation Δr is determined by a sum of several

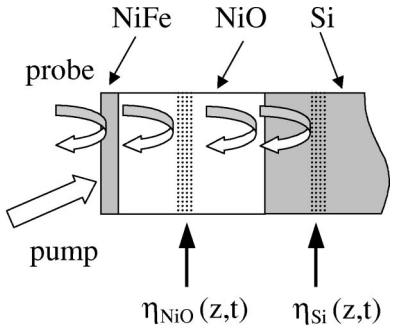

FIG. 1. Schematic diagram of the samples used in our experiments. The pump pulse excites the strain pulses from the NiFe side, which plays the role of the transducer. All the constant and acoustic induced reflectivities are displayed.

contributions due to the presence of the strain pulse in all the layers, which must be added to the unperturbed reflectivity r_0. In the simplest case when the sample consists of only the transducer and a transparent substrate, one obtains[1,22]

$$r_{total}=r_0+\Delta r=r_0+\beta(\epsilon_1,\epsilon_2)\int_0^\infty \Delta\epsilon(z,t)\ e^{2ikz}\ dz, \tag{1}$$

where $\Delta\epsilon=\Delta\epsilon_1+i\Delta\epsilon_2$ are the changes in the real and imaginary parts of the dielectric constant due to the compression wave $\eta(z,t)$, β is a constant that depends on the unperturbed dielectric constant, and $z=0$ at the transducer/film interface. For small changes of the dielectric constant $\Delta\epsilon(z,t)$, the measured transient reflectivity is proportional to

$$|r_{total}|^2 \approx |r_0|^2+2Re(r_0^*\Delta r), \tag{2}$$

and therefore linear in Δr. The optical phase factor in the integral of Eq. (1) is $2kz=(4\pi n_{probe}/\lambda_{probe})z$, where λ_{probe} and n_{probe} are the probe wavelength and the complex refractive index, respectively. If the strain field is decomposed into its Fourier components this phase factor will select the mode that fulfills the Bragg condition $2k=q$, where q is a wave vector of the longitudinal phonon spectrum. As for any radiating array, the width of the selection filter depends on the sample's effective length L, typically through a sinc function whose width in q space is $\Delta q_{filter}\approx 1/L$. The signal oscillates with a period given by $\tau=\lambda_{probe}/(2n_{probe}v_s)$,[3,22,24] which allows one, for example, to determine the refractive index if the speed of sound is known, or vice versa.

For a sample with more than one different layer after the transducer, both the excitation and detection processes are affected. Regarding the detection, the complete description of this problem has been layed out by Wright,[22] who considered the influence of the multiple reflections from all interfaces and strain pulses, in all layers. The variation of the optical thickness in each layer was also taken into account. In the treatment presented here the multiple reflections have not been considered, the reason being that the absorption in the NiO layer is not negligible, which reduces the contribution of multiple reflections,

$$\Delta r=\Delta r_{NiO}+\Delta r_{Si}, \tag{3}$$

where Δr_{NiO} is the contribution from the film and Δr_{Si} represents reflection off the strain wave within the substrate. It is important to note that in the contribution from the Si substrate there is an optical phase factor due to the round trip within the NiO layer. The contribution from the strain wave in the NiFe layer will later be seen to have no influence on the transient reflectivity.

We focus first on the contribution from the thin NiO layer, that has the form of the second term in Eq. (1), with the integration limited to L. As in the previous case the wave vector $q=2k$ is selected, this time out of a discrete spectrum. The probe pulse absorption is not negligible, but does not impede probing the underlying Si substrate. In both the NiO film and the Si substrate, the transient reflectivity will be determined by their respective refractive indexes and sound speeds: $\tau_j=\lambda_{probe}/(2n_j v_{sj})$.

As the NiO thickness L is small, both the forward- and back-propagating Fourier components of the strain field excited by the pump pulse must be considered,

$$\eta(z,t)=\sum_{q>0}\{\eta_q^+\exp[-i(\omega_q t-qz)] + \eta_q^-\exp[-i(\omega_q t+qz)]+cc\}, \tag{4}$$

where $\eta_q^\pm$ are the complex Fourier amplitudes, the frequencies are given by $\omega_q=qv_s$, with v_s being the speed of the longitudinal sound waves. The variation of the dielectric constants responsible for the reflectivity changes[16,22] are

$$\Delta\epsilon=\Delta\epsilon_1+i\Delta\epsilon_2=\left[\frac{\partial\epsilon_1}{\partial\eta}+i\frac{\partial\epsilon_2}{\partial\eta}\right]\eta(z,t), \tag{5}$$

proportional to $\eta(z,t)$. Introducing this expression into Eq. (1) for the reflectivity gives

$$\Delta r(t)\propto\theta(t)\ e^{i\varphi}\sum_{q>0}A(q)\ \{F(k,q)-F(k,-q)\}\sin(\omega_q t), \tag{6}$$

where φ is a phase that depends on the relative amplitudes of the induced changes in real and imaginary parts of the dielectric constant, $\Delta\epsilon_1$, and $\Delta\epsilon_2$, respectively; and $A(q)$ is an amplitude that depends on $\eta_q^\pm$. For strain pulses short compared to the round-trip time the amplitude $A(q)$ is a broad and smooth function. $F(k,q)$ is the filtering function and is given by

$$F(k,\pm q)=\frac{\exp[i(2k\pm q)L]-1}{i(2k\pm q)}, \tag{7}$$

and the filter's bandwidth is inversely proportional the sample's length: $\Delta q\propto 1/L$. The laser's bandwidth is of little influence since $\Delta k\ll\Delta q$, which means that the peak of the filter is at a well defined position.

The Fourier analysis presented above can be easily applied to the detection of the strain pulses in an absorbing sample, the difference being that the wave vector must now be considered as a complex quantity, the effective optical

length is smaller, and the filter function is broadened. The reflectivity signal is more localized in time because more frequencies are detected by the probe pulse.

For a transparent sample the number of modes that are detected, M, is given by the width of the filter function divided by the mode spacing, and is independent of L,

$$M = \frac{\Delta q|_{mode\ spacing}}{\Delta q|_{filter}} \approx \text{const}, \tag{8}$$

but the spacing between these modes in the frequency domain increases for thin samples, and the beating between the different modes may be observed. This is a different regime compared to most experiments previously reported on transparent films, where the samples are usually long, and opens the possibility to detect relative phases and determine relations between the changes induced by the strain pulse in the dielectric constants $\Delta\epsilon_1$ and $\Delta\epsilon_2$.

III. EXPERIMENT

The experimental setup consists of a time-resolved pump-probe system based on a femtosecond Ti:sapphire laser that generates pulses of 100 fs, at a repetition rate of 76 MHz, and a wavelength tunable within $\approx$50 nm of 800 nm. The excitation and probe pulses are focused by a 20$\times$ microscope objective at the sample and the relative delay between them is controlled by a stepping motor with 0.1-μm resolution. The pump pulse is mechanically chopped and the reflectivity changes are detected with a lock-in amplifier. The time-resolved reflectivity could be measured in either (i) a single wavelength scheme where the probe beam is at the same wavelength of the pump beam (λ_{pump}), or (ii) a dual wavelength scheme, where the probe is the second harmonic ($\lambda_{pump}/2$) of the pump beam. The probe pulses were roughly 1/10 of the pump pulses ($\approx 0.1\,nJ$) for the single-wavelength experiments and smaller than 1/100 for the dual-wavelength experiments. Typically, changes of one part in 10^4 of the reflectivity are measured.

The samples used in the measurements were originally designed for studying the magnetic exchange bias coupling between a ferromagnetic NiFe layer and an antiferromagnetic NiO layer,[18] and were prepared by dc magnetron sputtering in a Balzers/Pfeiffer PLS500 system. The nickel oxide layer was deposited on commercially available Si(001) after cleaning in ultrasound baths of acetone and ethanol for 10 min and drying in nitrogen flow. Above the NiO layer was deposited a film of $Ni_{80}Fe_{20}$, and no cover layer on the magnetic film was used. The base pressure of the system prior to deposition was 2.0×10^{-7} torr. The films were deposited in a 3.4×10^{-3}-torr argon atmosphere in the sputter-up configuration, with the substrate at a distance of 9 cm from the target. The purity of the NiO and NiFe target is 99.9%, and that of the argon gas is 99.999%. The films were deposited on the substrate at a temperature of 130 °C and the deposition rate was 0.7 /s. This rate was calibrated by measuring the frequencies of volume spin-wave modes in thicker films using Brillouin light scattering and confirmed by measurements in a surface profiler. The NiO film is oriented along the (111) direction, as determined from x-ray analysis. The nominal thickness of the NiO layer varied between 43.5 and 120 nm, while those of the NiFe layer varied between 10 and 30 nm.

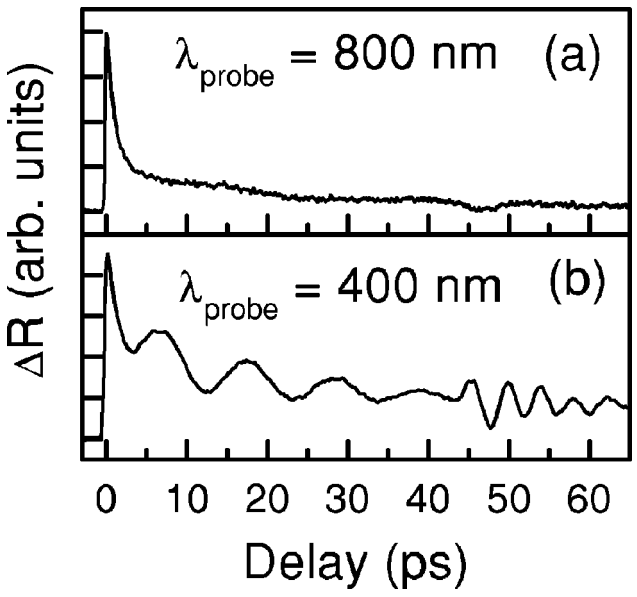

FIG. 2. (a) Transient reflectivity for a sample with a 10-nm NiFe transducer on a 274-nm-thick layer of NiO grown on a Si(001) substrate, with both pump and probe wavelengths at $\lambda = 800$ nm. (b) Pump at $\lambda_{pump} = 800$ nm and probe at $\lambda_{probe} = 400$ nm.

IV. RESULTS

This section describes our experimental results, starting with the differences in the observed signal when the probe wavelength is changed from the fundamental of the Ti:sapphire laser (800 nm) to its second harmonic (400 nm). Figure 2 displays the transient reflectivity in a sample where the NiFe layer has 10 nm, the NiO layer is nominally 120 nm thick and the probe wavelengths is either (a) 800 nm or (b) 400 nm. In the first case, the signal is dominated by an initial ultrafast decay, which is related to an electronic cooling process,[14] plus a slower decay possibly related to heat and electronic diffusion.[15] Figure 2(b) shows that when the probe wavelength is changed to 400 nm the detected signal is quite different: there are two distinct oscillations clearly observable. The fact that these oscillations are detected only when the second harmonic is used as a probe is due to the difference in the piezo-optic coupling: the second harmonic pulse is closer to the NiO gap, and also to the direct valence-to-conduction band transition in Si.[25]

The fast oscillation has a period of $\approx$4.4 ps, and it begins at a probe delay of 44 ps. The slow oscillation has a period of $\approx$11 ps, and initiates immediately after the pump pulse strikes the sample. As will be shown later we have identified that (a) the longer oscillation is related to the strain wave in the NiO layer, and (b) the faster oscillation is related to the silicon substrate. To substantiate this claim, measurements where the NiO thickness is varied have also been performed, keeping the probe wavelength (400 nm) and the transducer

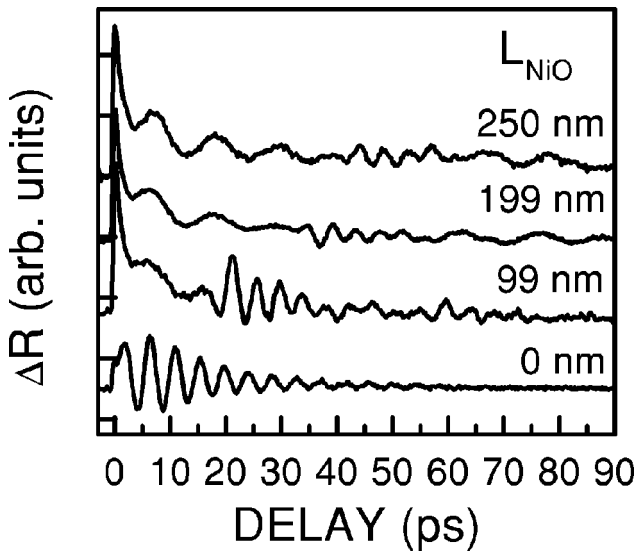

FIG. 3. Transient reflectivity for $\lambda_{probe}=400$ nm for samples with a 10-nm NiFe transducer, and a NiO thickness equal to 0, 99, 199, and 251 nm. The delay at which the fast oscillation begins depends linearly on the NiO layer, and occurs within the Si substrate.

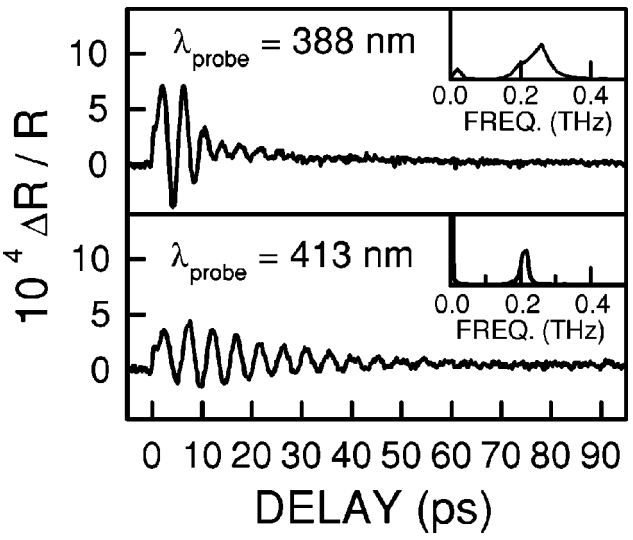

FIG. 4. (a) Transient reflectivity in a sample with no NiO layer, probing the strain pulses in Si, for a $\lambda_{probe}=388$ nm, with its Fourier transform shown in the inset. The peak is at $f\approx 0.26$ THz. (b) Same as in (a) but for $\lambda_{probe}=413$ nm, with the peak of the Fourier transform at $f\approx 0.21$ THz.

thickness (10 nm) fixed. The results are shown in Fig. 3, where it is clear that the periods of neither the slow or the fast oscillations change, but that the position at which the fast oscillations begins varies linearly with NiO thickness. Also, the relative amplitude of the fast oscillations increases with decreasing NiO thickness. This is due to the fact that, despite the absorption of light in this layer is much smaller than for the NiFe layer, it is still enough to change the amplitude of the probe wavelength that penetrates into the Si substrate.

If the thickness of the NiO layer is known, the sound velocity in the NiO layer can be obtained as $v_{NiO}=L/Td \approx 2.7$ nm/ps, which is quite different from the predicted bulk velocity in NiO, $v_{NiO(bulk)}=5-7$ nm/ps, depending on the crystalline orientation. We believe this discrepancy comes from the thickness calibration of our sample and therefore recalibrate the nominal thickness of our sample by assuming that the sound velocity in the NiO film is that of the bulk in the (111) direction, which has been measured[23] to be 6.2 nm/ps. This results in a recalibration of all NiO film thicknesses by a factor of 2.28, and it is these values that are quoted from this point on.

For the sample without the NiO layer we have varied the probe wavelengths around 400 nm. Despite both pump and probe wavelengths change in these measurements, we expect that the acoustic excitation process to be unchanged: it depends on the penetration depth in the NiFe layer, which is basically the same for the range of pump wavelengths used. Figure 4 presents the results for samples without the NiO layer, and for a 10-nm NiFe transducer. Figure 4(a). displays the transient reflectivity when $\lambda_{probe}=387.5$ nm, and the insert shows its Fourier transform. For this sample only the fast oscillation is present, with essentially no delay, indicating that this oscillation occurs in the Si substrate. Figure 4(b). shows the measurement for a $\lambda_{probe}=412.5$ nm. It is clear that both the oscillation frequency and the decay time of the signal depend on the probe wavelength: both the peaks and widths of the Fourier transforms vary with wavelength. The probe pulse is sensitive to the strain wave excited in the silicon layer, with the oscillation period determined by the real part of the refractive index and the decay time is determined by the imaginary part through the width of the filter function described by Eq. (7). Due to the strong absorption in Si for the range of wavelengths considered, the imaginary part of the photon wave vector, k, is quite large. From this data it is possible to obtain the dispersion of the real part of the refractive index, once the speed of sound for the (001) orientation of Si is known. Assuming $v_{Si(001)}=8.48$ nm/ps,[9] we obtain the dispersion curve shown in Fig. 5. These results are in good agreement with the known parameters for silicon.[25]

Figure 6 shows the results of measurements varying the probe wavelength for a sample with an 199-nm NiO layer and a 10-nm NiFe transducer, after subtraction of a double exponential decaying background, due to the contribution from the dynamics of electronic cooling[14] and heat and electronic diffusion.[15] Again the filter function selects the frequency of the detected oscillation, and there is a measurable change in the oscillation frequency with probe wavelength, as expected from predictions based on Eq. (5). We also notice that there is a small change in the phase of the oscillations around a delay of 67 ps, *independent of the probe wavelength*. This phase change is related to the round-trip time of the strain pulse in the NiO layer, and should also be present at half this delay, but cannot be seen here due to the fast oscillations from the Si substrate. From these data the complex refractive index in the NiO layer may be extracted, with the result for the real part of the refraction index dispersion displayed in Fig. 7, which is in reasonable agreement with bulk refractive index measurements for NiO.[26] Another

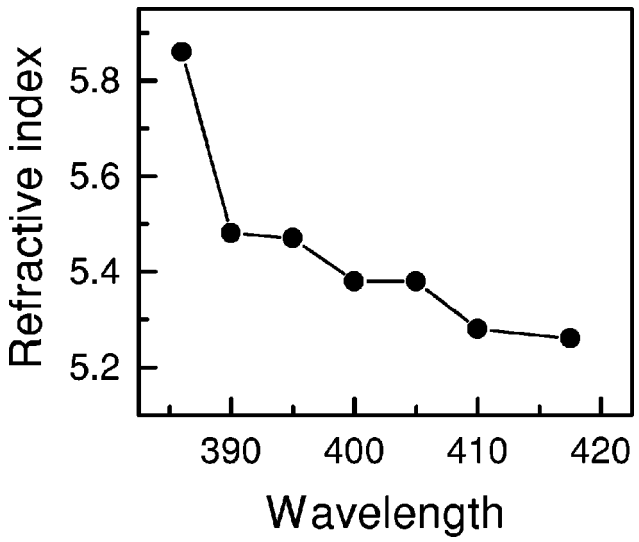

FIG. 5. Refractive index dispersion of Si obtained from the period of the fast oscillations with no NiO layer. The onset for direct valence to conduction-band transitions in silicon lies at $\approx$3.4 eV (364 nm).

point worth noting is that there is a phase change in the fast oscillations for $\lambda_{probe}=417.5$ nm, as indicated by the solid line in Fig. 6, located at the position where the fast oscillations begin. This wavelength dependent phase is not present in the measurements performed for the sample without the NiO layer, and therefore not related to changes in the piezo-optic coupling in Si.

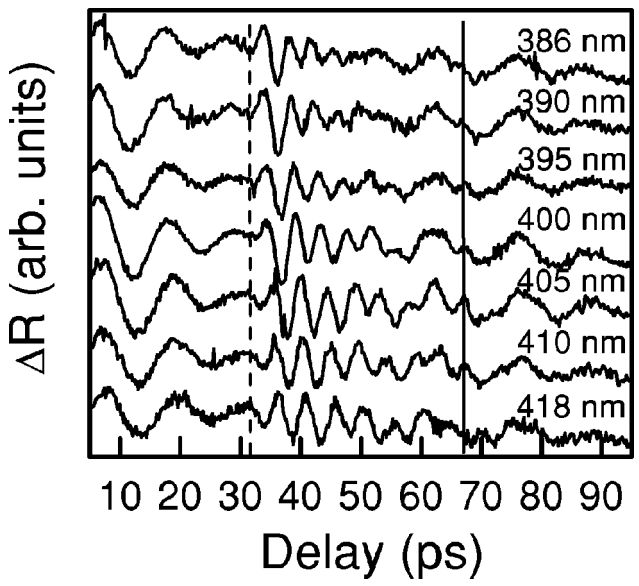

FIG. 6. Transient reflectivity for a sample with a 10-nm NiFe transducer, and a 199-nm NiO layer on a Si(001) substrate. The probe wavelengths varies between 386 and 418 nm. The dashed line indicates the begining of the fast oscillations, where a wavelength dependent phase is observed. The solid line illustrates the phase change that occurs at a probe delay of 67 ps, *that does not vary with probe wavelength*.

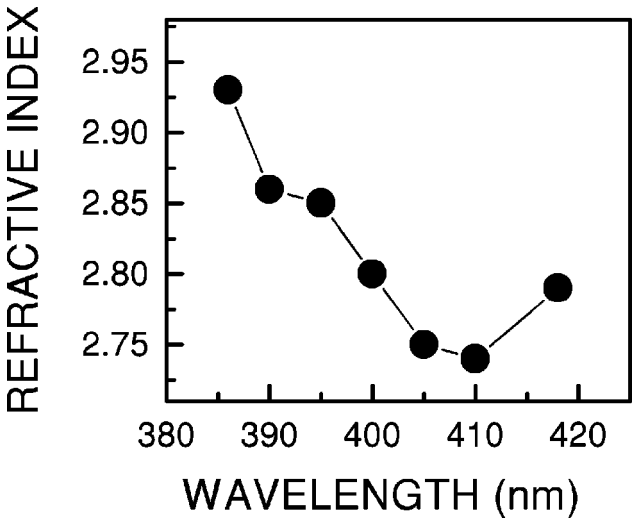

FIG. 7. Dispersion of the refractive index change for the NiO film, obtained from Fig. 6.

V. DISCUSSION

The results presented in the previous section are discussed in the light of Eq. (5). The transient reflectivity signal is proportional to the real part of $r_0^*\Delta r$, where r_0 is the unperturbed reflectivity due to all interfaces, including the pertinent optical phases of the back and forth travel to each interface, reminding that multiple reflections are not considered in our calculations. For the results presented in Fig. 6, for example, the fast oscillations occur in the substrate and the slow ones are due to the NiO film. The fast oscillations start when the strain pulse created in the NiFe transducer arrives at the NiO/Si interface. The penetration depth in the NiO film is of the same order of the layer's thickness and the probe pulse ''sees'' the strain wave over the whole film. The filter function is therefore determined mainly by the sample's length. Figure 8(a) shows the results for the numerical fit together with the experimental results for the 199-nm NiO layer, for $\lambda=400$ nm. We have included an empirical exponential decay time of 70 ps in Eq. (5) in order to account for the transmission losses of the strain pulse at the NiO/Si interface. A good comparison to the experimental data is also achieved if the amplitude of the oscillations are reduced by a constant factor after each reflection at the NiO/Si interface. Typically this reduction is of $\approx$ 40%. The fast oscillating contribution from Si has been omitted in the numerical fit in order to have a better view of the whole process, and a beating is clearly seen, involving the 5–6 different modes selected by the filter. In the calculations the penetration depth in the NiO layer is of the order of 50 nm, which is comparable to the sample's thickness. The effective sample length, due to absorption, is $L_{eff}=(1-e^{-\alpha L})/\alpha\approx 60$ nm, which does not change the filtering function much. An interesting aspect is that the position of the phase change observed in the slow oscillations around 67 ps, and reproduced in the simulation, depends only on the speed of sound and sample thickness.

Figure 8(b) displays the results for the numerical fit of the experimental data obtained *with the same parameters* used to

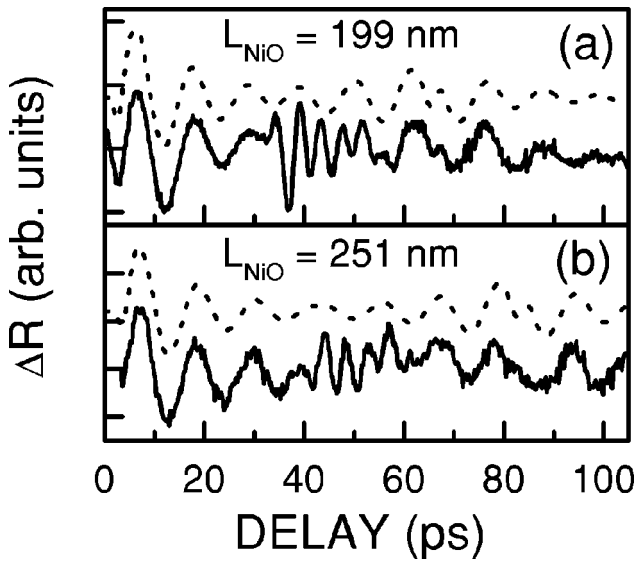

FIG. 8. (a) Numerical fit of the slow oscillation within a 199-nm-thick NiO film and $\lambda_{probe}=400$ nm. (b) Same as in (a) but for an 251-nm-thick NiO film, using the same parameters for the numerical fit. In the calculations we use $1/\alpha \approx 50$ nm for the penetration depth.

obtain Fig. 8(a): only the sample length L is changed to 251 nm in the simulation. Again, the agreement is quite good and the phase shift of the detected transient reflectivity is now observed for a greater delay time. From the numerical calculations it is clear that this phase shift is sensitive to the overall phase of the reflectivity, determined mainly by the ratio $\Delta\epsilon_1/\Delta\epsilon_2$, opening the possibility of measuring the real and imaginary contributions to the piezo-optic coupling.

Another interesting point is the wavelength dependent phase shift seen in the fast oscillations from the Si substrate. As the wavelength is varied from $\lambda_1=386$ nm to $\lambda_2=418$ nm, the delay of the first peak changes by about $\delta\tau \approx 2.5$ ps, which corresponds to a phase shift $\delta\phi \approx 2\pi\delta\tau/T_{Si} \approx 3.56$ rad or $\delta\phi \approx 2\pi(1-\delta\tau/T_{Si}) \approx 2.71$ rad, where $T_{Si} \approx 4.4$ ps is the (average) period of the fast oscillations. The origin of this phase is the propagation back and forth through the NiO layer, before the Si substrate, which introduces a wavelength dependent phase factor $\phi_{opt}=2(2\pi n_{NiO}/\lambda)L_{NiO}$. The calculated phase difference between the two wavelengths above, using the previously obtained refractive indexes, is $\delta\phi_{opt}=2(k_1-k_2)L_{NiO} \approx 2.3$ rad, which is reasonably close to the second estimate for $\delta\phi$. As the NiO layer thickness is close to one optical wavelength in this medium, this result serves as a double check for its refraction index measurements.

When the probe wavelength is changed from the fundamental to the second harmonic the magnitude of the piezo-optic coupling observed in both the NiO film and in the Si substrate varies quite dramatically. This must come from the detuning relative to absorption edges: in both materials the gap is around 3.4 eV[25] (in Si this is obviously the *direct* gap) and the second harmonic is closer to this value than the fundamental beam. One possibility is that due to electron-phonon coupling, the band edge of both these materials are displaced in the presence of a strain wave: $\Delta E_{gap}=\eta D$ where D is the optical deformation potential.[27] Variations in the band gap results in changes of the dielectric constants and there is expected to be a strong probe wavelength dependence in the coefficients $\partial\epsilon_1/\partial n$ and $\partial\epsilon_2/\partial n$ that appear in Eq. (5), for photon energies close to the band edge.[1] To check this possiblity it would be necessary to be able to tune the probe laser further higher into these transitions. There should be an observable change in the phase of the observed oscillations, if this is the mechanism responsible for the observed signal. Unfortunately, that is out the tuning range of our laser.

VI. SUMMARY

Ultrafast transient reflectivity measurements in a NiFe/NiO/Si structure have been performed. Significant changes are observed when changing the probe wavelength from $\lambda_{probe}=800$ to 400 nm, which are attributed to the greater proximity, in the second case, of the probe photon's energy to absortion edges in both NiO and Si. The influence of the probe penetration depth has been discussed in terms of the number of acoustic modes that are effectively detected, and the beating between the modes of a NiO film were observed, because of the small thickness of this film.

The refractive index dispersion curves for both Si and NiO have been obtained. The use of thin transparent films in picossecond ultrasonics opens the possibility to obtain quantitative information on the real and imaginary contributions of the dieletric constant to the coupling between light and sound waves.

ACKNOWLEDGMENTS

We acknowledge several discussions and suggestions from Professor J. R. Rios Leite. This work was supported by CNPq-PRONEX (Brazilian Agency).

[1] C. Thomsen, H.T. Grahn, H.J. Maris, and J. Tauc, Phys. Rev. B **34**, 4129 (1986).
[2] H.T. Grahn, H.J. Maris, J. Tauc, and K.S. Hatton, Appl. Phys. Lett. **53**, 2281 (1988).
[3] H.T. Grahn, D.A. Young, H.J. Maris, J. Tauc, J.M. Hong, and T.P. Smith III, Appl. Phys. Lett. **53**, 2023 (1988).
[4] H.T. Grahn, H.J. Maris, and J. Tauc, IEEE J. Quantum Electron. **25**, 2562 (1989).
[5] G. Tas, R.J. Stoner, H.J. Maris, G.W. Rubloff, G.S. Oehrlein, and J.M. Halbout, Appl. Phys. Lett. **61**, 1787 (1992).
[6] P. Basséras, S.M. Gracewski, G.W. Wicks, and R.J.D. Miller, J. Appl. Phys. **75**, 2761 (1994).
[7] B. Perrin, B. Bonello, J.-C. Jeannet, and E. Romatet, Physica B **219&220**, 681 (1996).
[8] N.-W. Pu, J. Bokor, S. Jeong, and R.-A. Zhao, Appl. Phys. Lett. **74**, 320 (1999).

[9] H.-Y. Hao and H.J. Maris, Phys. Rev. Lett. **84**, 5556 (2000).
[10] H.-Y. Hao and H.J. Maris, Phys. Rev. B **64**, 064302 (2001).
[11] G.L. Eesley, Phys. Rev. Lett. **51**, 2140 (1983).
[12] R.W. Schoenlein, W.Z. Lin, J.G. Fujimoto, and G.L. Eesley, Phys. Rev. Lett. **58**, 1680 (1987)
[13] S.D. Brorson, A. Kazeroonian, J.S. Moodera, D.W. Face, T.K. Cheng, E.P. Ippen, M.S. Dresselhaus, and G. Dresselhaus, Phys. Rev. Lett. **64**, 2172 (1990).
[14] C.K. Sun, F. Vallee, L. Acioli, E.P. Ippen, and J.G. Fujimoto, Phys. Rev. B **48**, 12 365 (1993); **50**, 15 337 (1994).
[15] G. Tas and H.J. Maris, Phys. Rev. B **49**, 15 046 (1994).
[16] A. Devos and C. Lerouge, Phys. Rev. Lett. **86**, 2669 (2001).
[17] A. Melikyan and H. Minassian, Chem. Phys. Lett. **331**, 115 (2000).
[18] J.R. Fermin, M.A. Lucena, A. Azevedo, F.M. de Aguiar, and S.M. Rezende, J. Appl. Phys. **87**, 6421 (2000).
[19] I. Hitovy, J. Huran, J. Janik, and A.P. Kobzev, Vacuum **51**, 157 (1998).
[20] I. Hitovy, J. Huran, L. Spiess, S. Hascik, and V. Rehacek, Sensors Actuators B **57**, 147 (1999).
[21] A. Azens, L. Kullman, G. Vaivars, H. Nordborg, and C.G. Granqvist, Solid State Ionics **113-115**, 449 (1998).
[22] O.B. Wright, J. Appl. Phys. **71**, 1617 (1992).
[23] J. Wang, E.S. Fisher, and M.H. Manghnani, Chin. Phys. Lett. **8**, 153 (1991)
[24] C. Thomsen, H.T. Grahn, H.J. Maris, and J. Tauc, Opt. Commun. **60**, 55 (1986).
[25] M. L. Cohen and J. R. Chelikowsky, *Electronic Structure and Optical Properties of Semiconductors*, Springer Series in Solid-State Sciences Vol. 75, 2nd ed., edited by M. Cardona (Springer-Verlag, Berlin, 1989).
[26] R.J. Powell and W.E. Spicer, Phys. Rev. B **2**, 2182 (1970).
[27] B. K. Ridley, *Quantum Processes in Semiconductors*, 2nd ed. (Clarendon Press, Oxford, 1988).